Crack Growth Behavior in a Composite Propellant with Strain Gradients—Part II

C. T. Liu*
Astronautics Laboratory, Edwards Air Force Base, California 93523

The crack growth behavior in a highly filled composite propellant with strain gradients was studied through the use of centrally cracked, wedge-shaped sheet specimen. The specimens were tested under a constant strain rate condition at room temperature. Two crack lengths were considered. The experimental data were analyzed to calculate the instantaneous stress intensity factor K_I and the associated instantaneous crack growth rate da/dt. In the data analysis, four data processing methods—the secant method, the modified secant method, the spline fitting method, and the total polynomial method—were considered. The effect of the data processing method and the time interval for crack length measurement on the accuracy of the calculated crack growth rate was investigated. In addition, the effect of the initial crack length, the nonuniform gross strain field, and the data processing method on the crack growth behavior was also investigated, and the functional relationship between the stress intensity factor and the crack growth rate was determined.

I. Introduction

IN designing a structural component, a thorough knowledge of the material properties of the engineering material and the pertinent failure criterion for a specific failure made is required. During past decades, the fracture mechanics approach has been used frequently as a failure criterion for high-strength materials. This approach is based on the assumption that the stress field in the immediate vicinity of a crack tip can be determined by the linear elastic fracture mechanics theory, provided nonlinear behavior is of limited extent. The influence of this stress field can be measured in terms of the stress intensity factor, which is a function of the applied load and the geometries of the crack and the specimen. According to the fracture mechanics approach, fracture occurs when the stress intensity factor attains the critical value, which is a material property to define the onset of brittle (unstable) fracture of the material. This fracture initiation criterion implies that a structure will fail as soon as a crack is initiated. It is based on the assumption that a crack, once it is initiated, will propagate at a very high speed and the structure will fail immediately. However, under certain loading conditions and certain geometrical configurations, subcritical cracks in a structural material can slowly extend and result in a time-dependent fracture process as well as fracture stress. Therefore, under this condition, a structure's useful life will be governed by the subcritical crack growth in the material. Thus, in an attempt to predict the ultimate service life of a structure and to use the material effectively, the failure criterion should include the crack propagation aspect of the subcritical crack growth.

As the requirement for rocket motor performance and reliability is advanced, the need to incorporate fracture mechanics in evaluating the propellant grain's structural integrity becomes more urgent. Before this can be accomplished, detailed knowledge of the characteristics of the crack growth behavior in a solid propellant is required.

Presented as Paper 85-0615 at the AIAA/ASME/ASCE/AHS 26th Structures, Structural Dynamics, and Materials Conference, Orlando, FL, April 15–17, 1985; received Jan. 2, 1986; revision received March 8, 1990; accepted for publication March 9, 1990.

*Project Manager. Member AIAA.

During the past years, a considerable amount of work has been done in studying the crack growth behavior in solid propellants under various loading conditions.[1-6] The basic approach is to determine the kinetics of the crack growth in terms of the relationship between the crack growth rate da/dt and the stress intensity factor K_I. The published data and derived functional relationship between da/dt and K_I were obtained by testing centrally cracked biaxial specimens under uniformly applied loading conditions. The effect of a nonuniformly applied gross strain field, which is a typical loading condition that a solid propellant grain will be subjected to under thermal and/or pressure loading conditions, on the crack initiation, the distribution of the strain field in the specimen, and the crack growth behavior in a composite solid propellant was investigated by Liu.[6]

In the present study, Liu's data were analyzed to determine the effect of the methods of da/dt calculation and the time increment for measuring the crack length on the accuracy of the da/dt calculation. In addition, the effect of nonuniform gross strain field on the subcritical crack growth expressed in terms of $\dot{a}$ (K_I) in the composite propellant was investigated.

II. Experimental Data

The experimental data collected by Liu[6] consists of crack length, load, and time, obtained by conducting crack propagation tests on crack wedge-shaped biaxial specimens. The length of the specimen was 8.0 in. and the thickness was 0.2 in. The width of the specimen varied symmetrically so that at the small end it was 1.5 in. wide, and at the large end it was 2.5 in. wide. Therefore, for a given load, this geometry produced a continuously varying strain field across the length of the specimen. Along the horizontal centerline of the specimen, two cracks of two lengths, 1.0 in. and 2.0 in., were cut through the center. The geometry of the specimen is shown in Fig. 1.

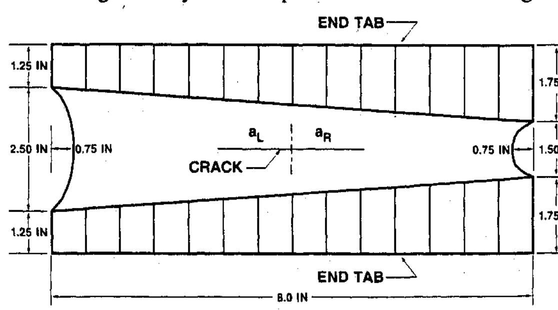

Fig. 1 Specimen geometry.

Crack propagation tests were conducted under a constant strain rate condition at room temperature. During the experiment, the crack length, the load, and the time were recorded. These data served as input to a computer program that calculated the crack growth rate and the stress intensity factor and then determined the functional relationship between these two parameters. A detailed description of the tests is shown in Ref. 6.

III. Data Reduction

The raw data obtained from the constant rate test were the two half-crack lengths, the right-side half-crack length a_r, and the left-side half-crack lengths a_l, which were measured from the center of the specimen; the time t and the load P, corresponding to the measured time. The raw data a_r and a_l were plotted as a function of time t in Figs. 2 and 3. These data were used to calculate the crack growth rate da/dt by four different methods. The methods considered were 1) the secant method, 2) the modified secant method, 3) the spline fitting method, and 4) the total polynomial method. A detailed description of the four methods is shown in Ref. 5 and in the following paragraph.

In the first method, known as the secant method, the crack growth rate was computed by calculating the slope of a straight line connecting two adjacent a vs t data points and assigning the average crack growth rate at a point midway between each pair of data points. The second method was the modified secant method and was done by averaging two adjacent growth rates, also obtained by the secant method, and assigning the averaged crack growth rate to the middle point of the three data points. The third method, the spline fitting method, fit a smooth continuous curve through a set of data points by a third-order polynomial together with the requirement of a continuous first and second derivative of the fitted function at the data point. The fourth method was the total polynomial method. This method involved fitting an nth-order polynomial to a set of data. The coefficients of the polynomial function were estimated by the method of least squares.

To determine the stress intensity factor at the crack tip, it is necessary to relate the load on the specimen to crack and specimen dimensions. A three-dimensional finite element computer code TEXGAP-3D[7] was used to determine the stress intensity factors as a function of the crack lengths for a given load P applied at the boundary of the specimen. The calculated mode 1 stress intensity factors K_{Ir} and K_{Il} at the right-side and the left-side tips were normalized with respect to the applied load P. Nonlinear regression analyses were conducted to generate two response surface equations, relating the dependent variables K_{Ir} and K_{Il} to the independent variables a_r and a. The finite element analyses of the cracked specimen as well as the generated response surface equations are shown in Ref. 6.

To avoid the time-consuming process of data reduction, a computer program was written to calculate the crack growth rate, based on the aforementioned four methods, and the stress intensity factor, based on the generated response surface equations. In addition, a subroutine, originally written by Virkler,[8] was incorporated in the program to determine the amount of error introduced into the crack propagation data for each of the four crack propagation rate calculation methods. This subroutine calculated the crack length as of function of time by integrating the estimated da/dt data and then comparing it with the original a vs t data. The relative error, expressed as the ratio of the difference between the integrated data and the original data, was calculated step by step, and the average of the relative errors was also calculated. By comparing these average incremental errors, the da/dt calculation method that results in the least amount of error can be selected. In the error analysis, the effect of the time interval Δt on the accuracy of the da/dt calculation was studied, and a total of five time intervals (t = 3, 6, 9, 12, 15 s) were considered. In the subsequent data analysis, only two methods of da/dt calculations, the secant method and the total polynomial method, and the optimum time interval Δt were used in processing the crack growth rate and the stress intensity factor. The results of the data analysis will be shown and discussed in the following paragraphs.

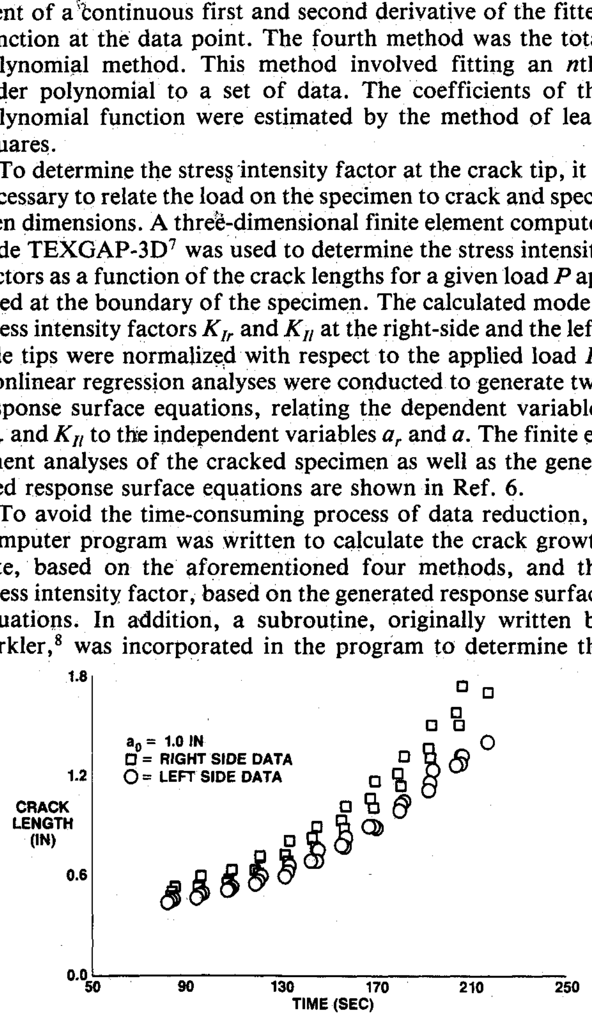

Fig. 2 Crack length vs time (a_0 = 1.0 in.).

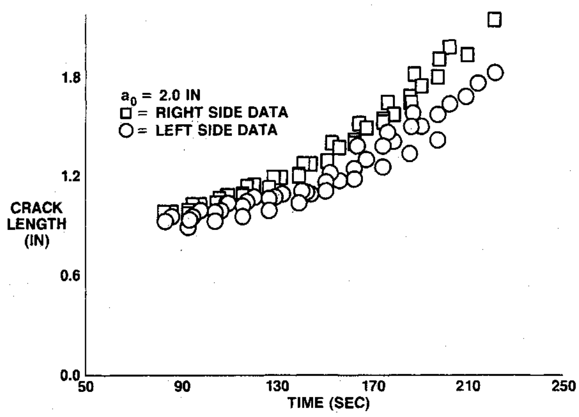

Fig. 3 Crack length vs time (a_0 = 2.0 in.).

IV. Results and Discussion

Crack growth rate determination requires an analysis of discrete data relating the instantaneous time t to the corresponding crack length a. The general problem encountered in determining crack growth rate is determining the derivative of a function $a = f(t)$ that is known only at certain data points. In addition, the inherent nonhomogeneous nature of a highly filled composite solid propellant will inevitably cause a considerably higher scatter in the measured data. Therefore, it is anticipated that a smooth and steadily increasing relationship between the crack growth rate da/dt and the time t is difficult to obtain and that different methods of da/dt calculation and different time increments for measuring the crack length may result in different solutions. It is the purpose of this study to investigate the influence of these parameters on the accuracy and scatter of the crack growth velocity da/dt. The results of the analysis are shown below.

The result of the error analysis is shown in Fig. 4 with the computational error plotted as a function of the method of the $\dot{a}$ calculation and the time interval Δt. The figure reveals that a definite trend exists between the computational error and the time interval Δt. For the four methods of the $\dot{a}$ calculation considered in this study, the computational error decreases with increasing Δt until it reaches a minimum value and then it has a tendency to increase as the Δt is further increased. The curves also indicate that method 1 introduces the least amount of error into the crack growth rate, followed by methods 3, 2, and 4. The differences between the computational error values associated with methods 1 and 3 are small when Δt is greater than 9 s. However, the computational error values for method 4 are significantly higher than those for the other three methods. This indicates that the inherent variability of the crack growth rate may be masked by the data's smooth action introduced by fitting a smooth polynomial curve through the

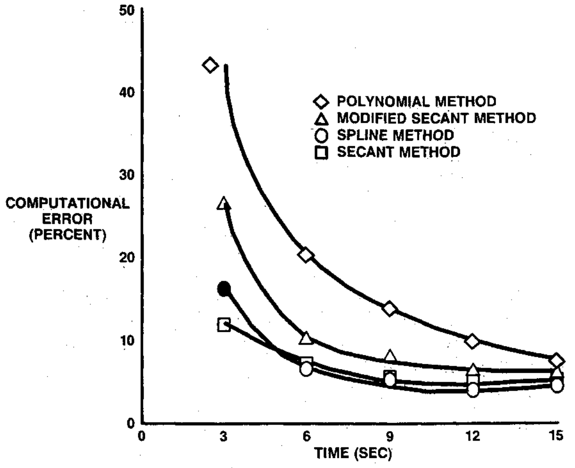

Fig. 4 Computational error vs Δt increment size.

discrete data points. Therefore, when selecting a method to calculate the crack growth rate from the raw experimental data, the accuracy and the scatter that are introduced into the calculated crack growth rate by the selected data processing method should be considered.

Based on the results of the error analysis, the secant method (method 1) and the 12-s time interval were used to analyze the crack growth data. For comparison, the polynomial method (method 4) was also used to analyze the data. The results of this analysis are presented and discussed in the following paragraphs.

The results of the data analysis, plotted as the stress intensity factor K_I, vs the crack extension Δa, are shown in Fig. 5. This figure has three regions, and it shows a similarity to the R curve observed for metallic and composite materials. In the first region, defined as the crack tip blunt stage, experimental data showed that the crack tip radius continually increased with increasing applied load and no crack extension took place. When the applied load reached a critical value for crack growth, the crack started to propagate, which defined the onset of the second region of the R curve. In this region crack growth was stable under an increasing load. The stable crack growth implied that after the first increment of the crack growth, an increment in the applied load was required for further crack growth. The amount of the increasing load was related to the slope of the R curve. In the second region, the slope of the R curve was positive and, initially, relatively steep. The steep slope implied that a relatively large increment of load was required to induce a small extension of the crack. As the stable crack grew continually, the relationship between the crack extension and the stress intensity factor changed successively. This was indicated by the continually changed slope of the R curve. The decrease in the slope of the R curve implied that the energy per unit extension required to continue crack propagation was decreased or that the increment of the crack extension per unit load was increased. The R curve was not expected to rise indefinitely. At some value of the crack length, the transition from region 2 to region 3 was completed. A careful examination of the experimental data revealed that the transition region was located approximately near the maximum applied load. This implied that region 3 was characterized by a continual decrease in the applied load with a continual increase in the crack length and a relatively constant value of the stress intensity factor. However, the crack was not driven at constant velocity, but instead it propagated at an accelerating rate.

Therefore, the onset of region 3 could be considered as the onset of the unstable part of crack growth. In this region, as observed in Fig. 5, the R curve also showed three different shapes, according to whether the slope of the R curve was greater than, equal to, or less than zero. However, it should be pointed out that the negative slopes of some of the crack growth resistance data were due to a large drop of the applied load, which was caused by the generation and the propagation of a second crack in the high-stress region at the right-side edge of the specimen, as mentioned in Ref. 6.

Referring to Fig. 5, the range of region 2 of the R curve encompasses an approximate range of K_I from 30 psi $\sqrt{\text{in.}}$ to 60 psi $\sqrt{\text{in.}}$ for both the right-side and the left-side crack growth data. This indicates that the value of the stress intensity factor that corresponds to the unstable crack growth is approximately two times larger than that required for the initiation of a stable crack growth. The figure also reveals the existence of scatter bands that embrace all the crack growth data and a relatively narrow band for the second region of the R curve. The small scatter of the test data in region 2 is probably well within the scatter of the experimental data due to the uncertainty of the measurements as well as the variability of the material properties. Therefore, in the second region of the R curve, the crack growth resistance curve can be assumed to be independent of the initial crack length and the magnitude of the nonuniform gross strain field.

A typical plot of the crack growth resistance data K_I and Δa on a log-log scale is shown in Fig. 6. The data indicate that a good correlation exists between log K_I and log Δa with a correlation coefficient equal to 0.916. The straight line relationship between log K_I and log Δa implies that a power law relationship exists between these two parameters.

Based on the above discussion, it can be stated that the quasistatic, stable crack growth in solid propellant is associated with a high resistance that is developed in the material. The increase in crack growth resistance with crack extension is the control factor for stability rather than the critical stress intensity factor for the onset of crack propagation. It is the crack growth resistance curve that measures the strength of the crack tip region of a growing crack. Therefore, in order to obtain a better understanding or to compare crack growth be-

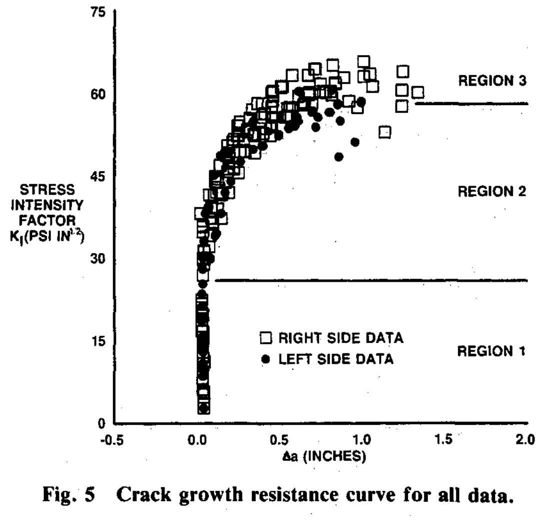

Fig. 5 Crack growth resistance curve for all data.

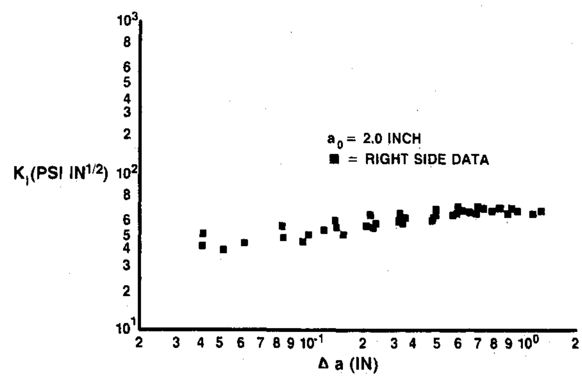

Fig. 6 Crack growth resistance curve (a_0 = 2.0 in.).

havior in solid propellants, the crack growth resistance curve (the R curve) is required. It should be pointed out that the crack growth resistance curve, shown in Fig. 6, was derived from experimental data obtained from experiments under a constant crosshead speed. Therefore, it may not be used to describe crack growth behavior under a different crosshead speed. To investigate the rate dependence of the crack growth resistance curve, additional tests need to be conducted for different crosshead speeds.

A typical plot of the crack growth rate $\dot{a}$ vs the time t for the two methods of the $\dot{a}$ calculation (the secant method and the polynomial method) is shown in Fig. 7. This figure clearly reveals that the method of the $\dot{a}$ calculation has a significant effect on the scatter of the calculated crack growth rate. Looking at Fig. 7, we recognize that a pronounced fluctuation of $\dot{a}$ is associated with the secant method. The magnitude of the fluctuation seems to decrease as the time is increased. Although the fluctuation of $\dot{a}$ occurs during the entire time range of crack growth, the general trend for the crack growth is that, on the average, the crack growth velocity increases with increasing time and the right-side crack propagates at a higher velocity than the left-side crack does. It is of interest to note that the two crack tips propagate out of phase with each other with different velocities. In other words, when the right-side crack grows fast, the left-side crack grows slow and vice versa. This kind of crack growth rate fluctuation does not occur when the polynomial method is used to calculate the crack growth rate. The smooth action introduced by the polynomial method results in a continuous smooth crack velocity curve. For both the right-side crack and the left-side crack, the crack growth velocity increases continually with increasing time, and the right-side crack always grows faster than the left-side

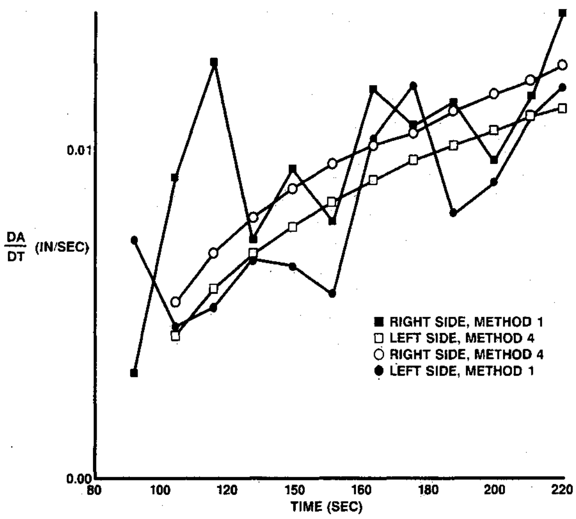

Fig. 7 Crack growth velocity vs time.

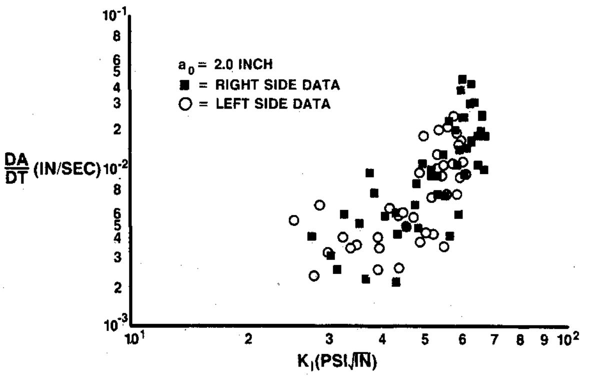

Fig. 8 Crack growth rate vs stress intensity factor (a_0 = 2.0 in., secant method).

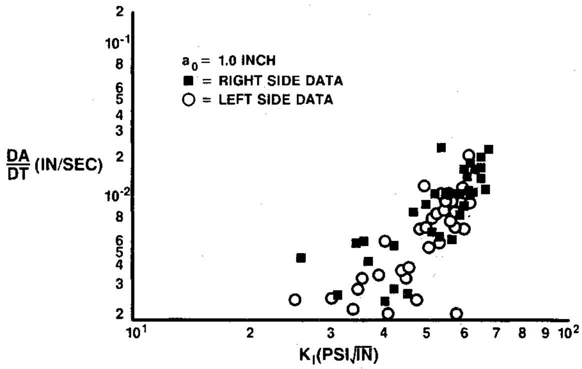

Fig. 9 Crack growth rate vs stress intensity factor (a_0 = 1 in., secant method).

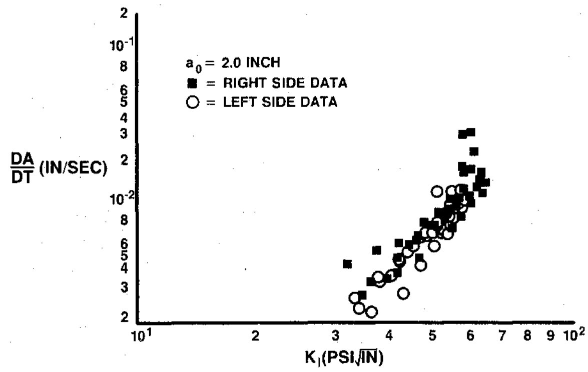

Fig. 10 Crack growth rate vs stress intensity factor (a_0 = 2.0 in., polynomial method).

crack. This is an expected phenomenon because the right-side crack propagates into a relatively higher gross strain field whereas the left-side crack grows into a relatively lower gross strain field. It is also of interest to note that the crack growth rate calculated by the secant method oscillates approximately around the smooth crack growth rate curve obtained by the polynomial method. This phenomenon is consistent with our expectations. Because, in the polynomial method, a higher-order polynomial function was selected to fit the discrete experimental data (crack length and time), the resulting crack length vs time curve became smooth. Therefore, it is reasonable to expect that, in general, the crack growth velocities calculated by the polynomial method may represent the mean crack growth rates with the crack growth rate calculated by the secant method oscillating around it.

The above discussion revealed two important aspects. First, note that with increasing time, the crack growth rate oscillates while the stress intensity factors increase. Second, the crack growth rate fluctuation is significantly affected by the method of the $\dot{a}$ calculation. Based on experimental evidence, in general, the crack does not grow in a continuous and smooth manner. During the crack growth process, crack growth velocity both accelerates and decelerates. Based on this experimental evidence, and in view of the nonhomogeneous nature of the solid propellant, the secant method appears to provide the best estimate of both the actual crack growth history and the actual crack growth velocity.

When the crack growth rate fluctuates, there will be no one-to-one correspondence between the crack growth velocity and the stress intensity factor. This contradicts current crack growth theory, which requires a unique relationship between the stress intensity factor and the crack growth rate. The lack of uniqueness between K_I and $\dot{a}$ raises two questions: to what extent the oscillation of $\dot{a}$ should be taken into account and how to present and use these data. How these questions are answered depends on how the gathered data will be used. If

Table 1 Summary of regression analysis

Data analyzed	Method of $\dot{a}$ calculation	Log C_1	C_2	R^a	S^b
Left side	1[c]	−6.66	2.60	0.707	0.215
Left side	4[d]	−7.25	2.98	0.945	0.074
Right side	1	−6.07	2.30	0.762	0.183
Right side	4	−6.47	2.54	0.959	0.054
Right and left sides	1	−6.87	2.77	0.73	0.219
Right and left sides	4	−7.01	2.87	0.906	0.107

[a]Coefficient of correlation. [b]Standard error of estimates. [c]Secant method. [d]Polynomial method.

one is interested in knowing the central tendency of the crack growth behavior, the fluctuation in $\dot{a}$ seems unimportant. However, if one is interested in determining the upper-bound limit on $\dot{a}$, the fluctuation in $\dot{a}$ should be considered in the data analysis. A more in-depth discussion of these options will be present later.

Plots of combined crack growth data (right side and left side) as K_I vs $\dot{a}$ for $a_0 = 1.0$ in. and $a_0 = 2.0$ in. are shown in Figs. 8–11. Looking at Figs. 8 and 9, we note that the right-side and the left-side crack growth data fall in the same scatter band, and there is no appreciable difference in these data. It seems that the effect of the nonuniform gross strain field on the crack growth behavior is negligible. A careful examination of the data in which $\dot{a}$ was calculated by the secant method reveals that, except for some unusual phenomena, for a given time, the stress intensity factor and the crack growth rate at the right-side crack tip are greater than those at the left-side crack tip. However, later the values of K_I and $\dot{a}$ at the left-side crack tip approach the earlier time values of K_I and $\dot{a}$ at the right-side crack tip. In other words, the crack growth behavior of the left-side crack has a tendency to approach the crack growth behavior of the right-side crack at a later time. It seems that crack growth data for the two sides may approach each other by shifting the data on a time scale. Therefore, when all data K_I and $\dot{a}$ are plotted together, the right-side and the left-side data overlap, and there is no appreciable difference between them. This is also true for the $a_0 = 1.0$ in. data shown in Fig. 9. Interestingly, a comparison of Figs. 8 and 9 shows that the two sets of data $a_0 = 1.0$ in. and $a_0 = 2.0$ in. are approximately encompassed by the same scatter band. This implies that the initial crack length as well as the nonuniform gross strain field considered in this study have no significant effect on the crack growth behavior. This is also true for the R curve shown in Fig. 5. Comparing Fig. 10 with Fig. 11 reveals that the same conditions also hold for the crack growth data derived from the polynomial method. Figures 10 and 11 also show that the scatter of the crack growth data is much narrower than the scatter patterns shown in Figs. 8 and 9.

Figures 8–11 show that the crack tends to propagate at a higher rate when the value of K_I is approximately equal to 60 psi $\sqrt{\text{in}}$. This value of K_I is the value at which the unstable crack growth starts or the point that corresponds to the onset of region 3 in the R curve shown in Fig. 5. In the early crack growth stage of Figs. 8 and 9, the crack growth data show a relatively large scatter. The scatter seems to decrease as the stress intensity factor increases. In other words, the data tend to coverge as the stress intensity factor increases. This phenomenon is similar to that reported by Liu[5] in his study of the statistical nature of crack growth behavior in solid propellants. It was found that the coefficient of variation of the crack growth rate decreased as the value of K_I increased. The method used to calculate $\dot{a}$ affected the value of the coefficient of variation for $\dot{a}$. The result of Liu's analysis indicated that the secant method and the polynomial method yield the largest and the smallest coefficient of variation values, respectively. This finding is consistent with the result of the statistical analysis of the present data, which will be shown later.

Based on Figs. 8 and 9, the data exhibit a relatively large scatter, especially in the early stage of crack growth. There are many factors that may contribute to the scatter of experimental data.[9] For a given testing condition and data reduction method, the variation in the test data can be attributed to the material's microstructure. On the microscopic scale, a highly filled composite propellant can be considered a nonhomogeneous material. When this material is strained, the different size and distribution of the filler particles, the variation in the bond strength between the particles and the binder, and the different cross linking density of polymer chains can all produce a highly nonhomogeneous local stress field. Also, this material may contain randomly spaced microvoids, incipient damage sites, and microcracks with statistically distributed size and directions. Therefore, the local material strength varies in a random fashion. Since crack growth behavior is controlled by the combination of local stress and local strength in varying combinations, it is expected that the crack growth data obtained from a number of tests will show a considerably larger scatter even though the testing conditions remained identical. Under this condition, the statistical method must be used to treat the test data so that the statistical variability of the measured data can be evaluated and the statistically based mean response and the upper-bound limit can be determined.

In this study, a linear regression analysis computer program was used to determine the functional relationship between the stress intensity factor K_I and the crack growth rate $\dot{a}$. The results show that a power law relationship exists between K_I and $\dot{a}$, which is consistent with the theoretical results obtained by Schapery[10] and Knauss[11] in their study of fracture of linear

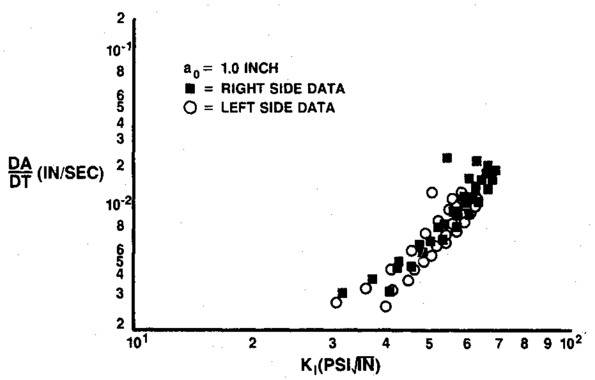

Fig. 11 Crack growth rate vs stress intensity factor (a_0 = 1.0 in., polynomial method).

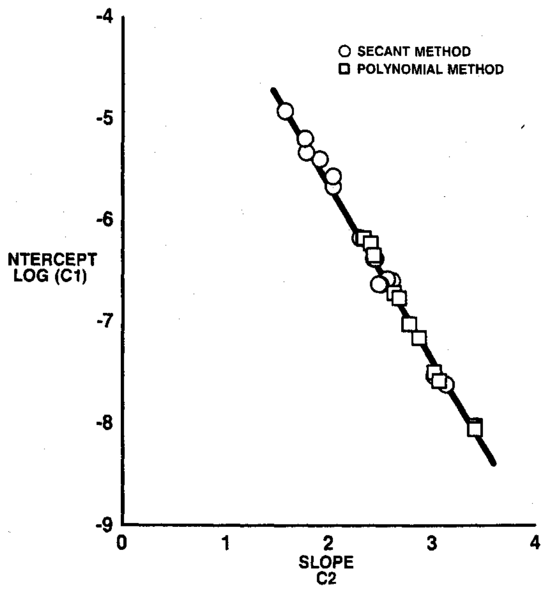

Fig. 12 Plot of C_1 and C_2 values from Eq. (1) (a_0 = 2.0 in.).

viscoelastic materials. Mathematically, it can be written as

$$\frac{da}{dt} = C_1 K_I^{C_2} \tag{1}$$

in which C_1 and C_2 are constants. The values of the coefficient of variation, the standard error of estimates, and the constants C_1 and C_2 are shown in Table 1. According to Table 1, the values of C_1 and C_2 for the two different methods of the $\dot{a}$ calculation differ from each other. Since C_1 and C_2 are empirically determined constants, it is expected that their values will vary from test to test as well as from one $\dot{a}$ calculation method to another.

In addition, the test data obtained from individual tests were analyzed to determine the values of the exponent and the intercept of Eq. (1). The determined values of C_1 and C_2 were not shown in Table 1; instead, they were plotted together with those shown in Table 1, in Fig. 12 as log C_1 vs C_2. It is clearly indicated that C_1 and C_2 are not constants but are mutually dependent and related through the equation

$$\log C_1 = A + BC_2 \tag{2}$$

where $A = -2.156$ and $B = -1.686$.

Equation (2) is derived from pairs of C_1 and C_2, which were obtained from all experimental tests data. Therefore, it is independent of the $\dot{a}$ calculation method, initial crack length, and the data sets used to derive C_1 and C_2. The existence of Eq. (2) implies that all straight lines relating to Log $\dot{a}$ and Log K_I, obtained from the regression analysis, converge and meet at a point. In other words, a pivotal point exists about which these lines rotated. The coordinates of the pivotal point can be determined from the two constants A and B in Eq. (2). Since C_1 and C_2 are related through Eq. (2) and the slope of Eq. (2) is negative, the decrease in C_1 will result in an increase in C_2. Therefore, when using Eq. (1) to predict $\dot{a}$ for a given K_I, a different value of C_2, shown in Table 1, does not necessarily result in a large difference in the value of $\dot{a}$. A simple calculation of crack growth rate, using Eq. (1) and C_1 and C_2 values from Table 1, can show that the difference in the calculated values of $\dot{a}$ are not large for a range of values of K_I (30 psi $\sqrt{\text{in.}}$ $\leq K_I \leq$ 60 psi $\sqrt{\text{in.}}$), especially at large values of K_I. The results also indicate that the method used to calculate $\dot{a}$ has a negligible effect on the predicted values of $\dot{a}$. Therefore, it can be stated that the $\dot{a}$ calculation method, the initial crack length, and the nonuniform gross strain field have no significant effect on the central tendency of the crack growth behavior as defined by the regression equations. However, from Table 1, the value of the standard error of estimate associated with the secant method is approximately three times as large as that associated with the polynomial method. This indicates that the $\dot{a}$ calculation method can also contribute to the scatter of the crack growth data.

V. Conclusions

The principal conclusions that may be derived from the results of this work under the conditions considered in this study are the following:

1) The method of the $\dot{a}$ calculation has a significant effect on the scatter but has a negligible effect on the central tendency of the crack growth data.

2) There is an optimum Δt measurement increment that will minimize the error in the $\dot{a}$ calculation.

3) The crack growth resistance curve is independent of the initial crack length.

4) A considerable amount of stable subcritical crack growth occurs before the onset of the unstable crack growth.

5) The initial crack length and the nonuniform gross strain field have no significant effect on crack growth behavior.

6) A power law relationship exists between the stress intensity factor K_I and the crack growth rate $\dot{a}$ and the equation is shown below:

$$\dot{a} = C_1 K_I^{C_2}$$

7) C_1 and C_2 are mutually dependent.

Acknowledgments

The work was supported by the Office of Scientific Research, Air Force Systems Command. The author expresses his appreciation to W. G. Knauss of the California Institute of Technology for his helpful comments and to S. Lin and B. Hunt for their assistance.

References

[1]Beckwith, A. W., and Wang, D. T., "Crack Propagation in Double-Base Propellants," AIAA Paper 78-170, Jan. 1978.

[2]Francis, E. C., Carlton, C. H., and Thompson, R. E., "Predictive Techniques for Failure Mechanisms in Solid Rocket Motors," UTC/Chemical Systems Div., San Jose, CA, AFRPL-TR-79-87, 1979.

[3]Liu, C. T., "Crack Propagation in an HTPB Propellant," *1980 JANNAF Structures and Mechanical Behavior Subcommittee Meeting,* Chemical Propulsion Information Agency, Applied Physics Lab., Laurel, MD, CPIA Pub. 311, Vol. I, March 1980, pp. 193–205.

[4]Dengle, D. H., Kornblith, J. S., and Hunston, D., "Fracture Behavior of Crosslinked Double Base Propellants," *1989 JANAF Structures and Mechanical Behavior Subcommittee Meeting,* Chemical Propulsion Information Agency, Applied Physics Lab., Laurel, MD, CPIA Pub. 351, Dec. 1981, pp. 129–140.

[5]Liu, C. T., "Variability in Crack Propagation in a Composite Propellant," AIAA Paper 83-1015, May 1983.

[6]Liu, C. T., "Crack Growth Behavior in a Composite Propellant with Strain Gradients—Part I," AIAA Paper 84-1294, June 1984.

[7]Kathiresan, K., and Atluri, S. N., "Three-Dimensional Homogeneous and Bi-Material Fracture Analysis for Solid Rocket Motor Grains by a Hybrid Displacement Finite Element Method," Georgia Inst. of Technology, Atlanta, GA, AFRPL-TR-78-65, 1978.

[8]Virkler, D. A., "The Statistical Nature of Fatigue Crack Propagation," M.S. Thesis, Purdue Univ., West Lafayette, IN, 1978.

[9]Clark, W. G., Jr., and Hudak, S. J., Jr., "Variability in Fatigue Crack Growth Rate Testing," *Journal of Testing and Evaluation,* Vol. 6, No. 3, 1975, pp. 454–476.

[10]Schapery, R. A., "On a Theory of Crack Growth in Viscoelastic Media," Texas A&M Univ., College Station, TX, Rept. MM 2763-73-1, March 1973.

[11]Knauss, W. G., "Delayed Failure—The Griffith Problem for Linearly Viscoelastic Materials," *International Journal of Fracture Mechanics,* Vol. 6, March 1970, pp. 7–20.

David H. Allen
Associate Editor